Journal of Hydrology 643 (2024) 131934

Contents lists available at ScienceDirect

Journal of Hydrology

journal homepage: www.elsevier.com/locate/jhydrol

Research papers

Snow simulation for the rangeland hydrology and erosion model

Patrick D. Broxton[a,*], David C. Goodrich[b], D. Phillip Guertin[a], C. Jason Williams[b], Carl Unkrich[b], Mariano Hernandez[a], Andrew Fullhart[b], Carrie-Ann Houdeshell[c], Mark Seyfried[d], Loretta Metz[e]

[a] School of Natural Resources and the Environment, The University of Arizona, United States
[b] USDA-ARS Southwest Watershed Research Center, United States
[c] USDA-NRCS Resource Inventory and Assessment Division, CEAP-Grazing Lands, United States
[d] USDA-ARS Northwest Watershed Research Center, United States
[e] USDA-NRCS Soil Health Division, United States

ARTICLE INFO

This manuscript was handled by Marco Borga, Editor-in-Chief, with the assistance of Kelly Kibler, Associate Editor

Keywords:
Snow
Erosion
Overland flow runoff
Rangelands
Hydrologic modelling
RHEM

ABSTRACT

In the western US, most rangelands receive snowfall. Yet, a commonly used tool to assess rangeland's vulnerability to erosion, the USDA's Rangeland Hydrology and Erosion Model (RHEM) is run using long-term simulated climate inputs that assumes that all precipitation occurs as rainfall. This can be problematic for areas that receive heavy snowfall or substantial rain-on-snow events. In this research, we have developed an efficient snow module for RHEM, called RHEM-Snow, which partitions precipitation between rainfall and snowfall, simulates snowpack accumulation and ablation, and passes net water input (consisting of rainfall, snowmelt, or both) to RHEM. In some areas, the inclusion of the snow module can reduce annual overland flow runoff and erosion estimates by more than 20 % of the total annual overland flow runoff and erosion produced without the snow module (or by as much as 10–50 mm/year for overland flow runoff or >100 kg/ha-yr for erosion). The reclassification of precipitation events from rainfall in RHEM to snowfall in RHEM-Snow tends to reduce overland flow runoff and erosion, but this reduction can be partially counterbalanced by increases from snowmelt and rain-on-snow. However, hydrologic responses to rain-on-snow events can either be enhanced or muted depending on the characteristics of the storm and the snowpack, as sometimes the snowpack can absorb the precipitation inputs, and sometimes snowmelt enhances the precipitation inputs. Because of this mixed impact, the average difference in erosion caused by rain on snow events is relatively small compared to corresponding events where only the liquid phase is considered. Further study is needed of the complex erosion processes under snowpack and frozen soil/variable saturation conditions. Overall, RHEM-Snow provides more realistic timing and magnitude of overland flow runoff and erosion in cold environments, better satisfying the conditions for RHEM applications.

1. Introduction

Minimizing water-driven soil loss is critical for maintaining the productivity of rangeland ecosystems (Havstad et al., 2009). Rangeland degradation through soil loss can adversely affect the ability of rangelands to support healthy ecosystems and decrease their ability to sustainably produce goods and services. Such degradation is potentially more likely in the future as the climate warms, leading to an enhanced hydrologic cycle and potentially more extreme storms (Nearing et al., 2004; Walthall et al., 2012; Zhang et al., 2012). As such, land managers need reliable models to predict runoff and soil loss (Flanagan et al., 2001). One such model, the Rangeland Hydrology and Erosion Model (RHEM), is capable of simulating overland flow runoff, soil erosion, and sediment delivery at the hillslope scale for disturbed and undisturbed rangelands (Al-Hamdan et al., 2017; Nearing et al., 2011). RHEM has been widely used to characterize the hydrologic vulnerability of hillslopes to soil loss associated with vegetation degradation (Hernandez et al., 2016; Williams et al., 2022), and it is a web accessible tool to help resource managers understand potential runoff and erosion rates under various land management scenarios (Hernandez et al., 2015; Williams et al., 2016).

Despite its wide adoption, one of the major limitations of RHEM is that it is designed to predict overland flow runoff and erosion due to rainfall events and does not consider mixed-phase precipitation. RHEM

* Corresponding author at: School of Natural Resources and the Environment, The University of Arizona, 1064 East Lowell Street, Tucson, AZ 85721, United States.
E-mail address: broxtopd@arizona.edu (P.D. Broxton).

https://doi.org/10.1016/j.jhydrol.2024.131934
Received 28 November 2023; Received in revised form 22 July 2024; Accepted 24 August 2024
Available online 7 September 2024

treats all precipitation events as rainfall, regardless of whether the temperature is cold, and the event should be regarded as snowfall. For many rangelands, consideration of precipitation events as rainfall is not a wrong assumption if intense precipitation occurs primarily as rainfall during the summer months (e.g. during summertime thunderstorms). However, some rangelands experience substantial snowfall during the winter season, especially at higher latitudes and/or elevations. In these areas, misclassifying snowfall as rainfall and not considering the impact of snow on the ground during rain-on-snow (ROS) events can substantially impact resulting runoff and erosion estimates (Marks et al., 2001; Nayak et al., 2010; Seyfried and Wilcox, 1995).

In general, snow changes the timing of hydrological inputs, storing precipitation from winter storms and later releasing the water as snowmelt. Commonly, snowmelt occurs relatively slowly, resulting in little hillslope erosion in most cases, though this is not always true, especially when the soil is frozen or partially frozen (Wu et al., 2018). Conversely, some wintertime precipitation events can cause substantial hillslope erosion if they have high enough intensity or are of long duration (Wade and Kirkbride, 1998). For example, atmospheric rivers (ARs) can bring large amounts of rain and snow to the western US, with some areas receiving more than half of wintertime precipitation from just a few events (Demaria et al., 2017; Dettinger et al., 2011). Incorrectly classifying these events at higher elevations (where snow occurs) as rainfall could lead to overestimates of the amount of runoff and erosion because the water would instead accumulate as snow and may melt more slowly at a later date. The impact of this misclassification, though, has not been quantified for hillslope erosion on rangelands.

Rain-on-snow can have various impacts on runoff and erosion, depending on atmospheric conditions, snowpack mass and energy content, and soil moisture/frozen ground. In some cases (e.g. if snowpack is cold and/or deep), the snowpack can absorb some of the rainfall, thus reducing the immediate hydrological impact of the precipitation event. However, other snowpacks cannot (e.g. if they are shallow or close to isothermal). Instead, rainfall on these snowpacks either percolates through the snowpack, or if it does freeze, the latent heat release associated with freezing causes a substantial amount of snowmelt (Wever et al., 2014). In addition, these events can be accompanied by an increase in longwave radiation (Mazurkiewicz et al., 2008), and there can be an efficient transfer of energy between the atmosphere and snowpack during ROS events, especially in open areas (Marks et al., 1998; Marks et al., 2001).

In addition to ROS events, there are a variety of underlying processes that can result in complex runoff generation and erosion in cold environments, but these processes are challenging to incorporate into a mathematical model. For example, freeze–thaw cycles can enhance erosion by loosening soil aggregates and causing higher runoff when the soil is frozen or partially frozen (Blackburn et al., 1990; Seyfried and Flerchinger, 1994; Wei et al., 2019). Other processes such as snow gliding (i.e., the slow movement of snowpack down a slope) can also be significant drivers of erosion (Meusburger et al., 2014; Wei et al., 2019). These processes deserve additional research and a modeling framework in which they may be incorporated. An important first step, though, is having a snow model that reasonably predicts water inputs from snowmelt using the information available to existing erosion models.

In this study, we developed a snow module for RHEM that enables us to simulate snow accumulation and melt. The snow module keeps track of the evolution of snowpack through the winter as well as the rainfall and snowmelt inputs to drive the event-oriented runoff and sediment transport model in RHEM. It also satisfies the fundamental computational and logistical constraints of coupling to the RHEM model (i.e. being forced with hundreds of years of stochastically generated daily weather data in a user-driven environment where model execution must be fast). The objectives of this paper are to 1) describe the snow module and its integration with RHEM, 2) evaluate its performance against observed hydrological data, and 3) assess the impact that it has on liquid water inputs (LWI), locally generated overland flow runoff (Q), and erosion (E) estimates from RHEM.

2. Methods

2.1. Model description

The snow module in RHEM-Snow is a computationally efficient hybrid between an energy balance and degree-day snowmelt model. It has separate layers representing the snowpack and soil, and a thin surface layer to compute radiative and turbulent exchanges with the atmosphere. The model codes developed in this study (in Python and Fortran) can run multiple hundred-year fully coupled simulations for a single site in a few minutes using a single processor. This computational efficiency means that the model can run in an on-demand fashion, so that it could be included in a decision support tool like the RHEM web tool (https://dss.tucson.ars.ag.gov/rhem/).

Like a mass and energy balance snowmelt model, the snow module in RHEM-Snow keeps track of the continuous mass and energy balance of the snowpack:

$$\frac{dSWE}{dt} = P_s + P_r - E - M \tag{1}$$

$$\frac{dcc}{dt} = Q_n + Q_h + Q_e + Q_g + Q_p + Q_m \tag{2}$$

where $\frac{dSWE}{dt}$ is the change in snow water equivalent per day, $\frac{dcc}{dt}$ is the change of cold content per day, P_s is snowfall, P_r is rainfall, E is sublimation, M is liquid water leaving the snowpack, and Q_n, Q_h, Q_e, Q_g, Q_p, and Q_m are, net radiation, sensible heat flux, latent heat flux (i.e. sublimation to/from the snowpack), ground heat flux, heat flux from precipitation (which considers sensible heat transfer from falling precipitation as well as latent heat transfer if liquid precipitation freezes to the snowpack), and heat due to phase change during melt/freezing. Note that all terms on the right sides of Eqs. (1) and (2) are mm/day and J/(m^2-day), respectively. In addition, the snow module accounts for attenuation/enhancement of solar radiation due to topography, temporally variable albedo and snow density, and sublimation of intercepted snow. Snow albedo is parameterized as a simple exponential decay since the time of last snowfall (Broxton et al., 2015), and snow density is modeled using an equation that densifies snow based on age of snowpack, overburden, and liquid water in the snowpack (Goodrich et al., 2023). Interception, canopy snow storage, sublimation of intercepted snow, snow unloading, and melt-drip from the canopy is modeled using the methodology in Liston and Elder (2006). RHEM-Snow, along with its documentation can be downloaded at https://github.com/ARS-SWRC/RHEM-Snow. Model equations can be found in Goodrich et al. (2023). Equations for most terms in Eqs. (1) and (2) are fairly standard, but a couple of model formulations (Eqs. (3) and (4)) that make RHEM-Snow unique are described in detail below.

Given its computational constraints, there is a simplification regarding snow surface temperature to facilitate faster model performance than a more detailed energy balance snow model might have. Namely, instead of solving for snow surface temperature iteratively, it is estimated as a function of air temperature, radiation, and relative humidity, which we determined empirically at a field site in Arizona (referred to below as Site S5):

$$T_s = T_a + 0.0258 \times (Q_{sn} + Q_{li}) + 0.0648 \times RH - 14.5601 \tag{3}$$

where T_s (°C) is the snow surface temperature, T_a (°C) is the air temperature, Q_{sn} (W/m^2) is net (incoming-outgoing) solar radiation, Q_{li} (W/m^2) is incoming longwave radiation, and RH (%) is the relative humidity. This model estimates the snow surface temperature well both at the Arizona site where it was developed, as well as other areas with independent measurements. For the Arizona site, it predicts surface temperature of snow with an R^2 of 0.95 and an RMSE of 0.9 °C, and for 5 flux tower sites located in the Reynolds Creek Experimental Watershed in Idaho, it predicts snowpack temperatures with R^2s ranging from 0.85 to 0.93 and RMSEs ranging from 1.1 to 2.0 °C (Fig. S1).

Like RHEM, RHEM-Snow is forced with 300 years of daily CLImate GENeration [CLIGEN; Nicks et al. (1995)] weather generator data. CLIGEN produces daily estimates of precipitation, temperature, dewpoint, wind, and solar radiation for individual geographic points. CLIGEN input parameters are derived from over 2600 high-quality, long-term (>30 years), meteorological stations in the United States and recently with near global coverage at a 0.25° spatial resolution (Fullhart et al., 2024; Srivastava et al., 2019). However, we have also included the capability to force RHEM-Snow with user-generated forcing datasets representing real observations. This allows for offline testing of the snow module with observed weather data (see Section 2.2).

LWI (rainfall and snowmelt) from the snow module is used to drive the hydrologic model that simulates overland flow in RHEM. RHEM is an event-oriented model that simulates infiltration, Q, and E resulting from precipitation events at high temporal frequency (Hernandez et al., 2017). RHEM (without the snow module) is forced with disaggregated CLIGEN daily precipitation, including time to peak intensity, peak intensity, and storm duration at a specific location. With this information, a sub-daily storm hyetograph can be derived using a double exponential function (Wei et al., 2007).

The double exponential function was selected after extensive testing (Lane and Nearing, 1989; Zhang and Garbrecht, 2003), as it was found to produce good runoff predictions in natural watersheds. For example, for the cases tested by Lane and Nearing (1989), the overall goodness of fit of the computed runoff volume and peak runoff rate using the disaggregated rainfall intensity was good when compared to runoff computed with the observed rainfall intensity: using the disaggregated rainfall as input to a calibrated infiltration-runoff model explained some 90 % of the variance in runoff computed using the observed rainfall. Note also that watersheds in rangeland areas tend to have small rainfall-runoff ratios [for example, the four range sites within the Long Term Agroecosystem Research network have runoff-rainfall ratios ranging from 0 to 0.11 (Baffaut et al., 2020)], and under these conditions, it is generally less important to closely reproduce the observed hyetograph from the disaggregated daily CLIGEN outputs because of the substantial attenuation of rainfall storm depth and temporal variability in the transformation of rainfall to runoff.

RHEM-Snow uses the same method (double exponential function) to disaggregate rainfall inputs, but it uses a different method to disaggregate snowmelt inputs, which have very different diurnal intensity patterns, with peaks occurring during the afternoon. Snowmelt inputs are disaggregated using a beta function (Webb et al., 2017):

$$FDM(t) = t^{\alpha-1}(1-t)^{\beta-1}\frac{\Gamma(\alpha+\beta)}{\Gamma(\alpha)\Gamma(\beta)} \tag{4}$$

where *FDM* is the fraction of daily melt Γ is the gamma function, t is the time of day (as a decimal between 0:00 and 23:00, and α and β are fitting parameters. This function was shown by Webb et al. (2017), using snow pillow data, and contextualized with soil moisture data, to be able to fit the diurnal cycle of fractional daily melt measurements. This function creates a single snowmelt peak during the daytime, and similar to Webb et al. (2017), we use fitting parameters such that the peak occurs in the late-afternoon, near the time of peak heating.

To simplify the combination of inputs, all LWI inputs are disaggregated to a 5-min timestep in RHEM-Snow. When there is both snowmelt and rainfall (e.g. which occurs on days with ROS), snowmelt is added to the rainfall input that percolates through the snowpack. The amount of water that percolates through the snowpack during the ROS event depends on the thermodynamic properties of the snowpack (i.e. the cold content), the rainfall amount, and the energy exchange that occurs during the event. To match how events are simulated in RHEM, each day's net water input is regarded as a single "event", and initial conditions (e.g., prescribed initial soil moisture) are the same as in RHEM.

2.2. Evaluation of the snow module

RHEM-Snow's snow module is evaluated using two tests: first, in order to determine the effectiveness of the snow module to reproduce in-situ snowpack measurements when forced with observed weather data, we evaluate the model deterministically, where the model is forced with observed weather station data at five field sites (3 in Idaho and 2 in Arizona) and evaluated against in situ snowpack measurements at these sites. Second, to demonstrate that the snow model still performs well in the context that the RHEM-Snow is run (i.e. forced with CLIGEN weather generator data), we also evaluated the model stochastically, where the model is forced with 300 years of CLIGEN data at the 1199 sites in the western US (Srivastava et al., 2019) and evaluated with the climatological distribution of snowpack properties from the University of Arizona Snowpack Data (Broxton et al., 2019a), which includes daily SWE maps covering the entire conterminous US at 4 km resolution since 1981.

For the deterministic simulations, we implemented the model at two field sites in central Arizona's highlands, as well as three sites in the USDA Agricultural Research Service (USDA-ARS) Reynolds Creek Experimental Watershed (RCEW) in Idaho (Sites S1–S5 in Fig. 1). The sites at RCEW include both sheltered (which has deeper snow; Site S1) and exposed (which has less deep snow; Site S2) snow measurement locations at a high elevation site with a seasonal snowpack (called Reynolds Mountain East), as well as another lower elevation site with an ephemeral snowpack (called Lower Sheep Creek; Site S3) (Marks et al., 1998; Reba et al., 2011; Seyfried et al., 2018; Seyfried and Wilcox, 1995). The sites in Arizona also have contrasting seasonal vs. ephemeral snowpacks (Broxton et al., 2019b; Dwivedi et al., 2023), though temperatures at these sites are generally warmer than those at RCEW. The seasonal snowpack site in Arizona (Site S4) is at the Maverick Fork SNOTEL (Site #617), in the White Mountains of Eastern Arizona, and the ephemeral snowpack site (Site S5) is at the Baker Butte SNOTEL (Site #308), which is located along the Mogollon Rim in central Arizona. These sites were chosen because they have contrasting ephemeral and seasonal snowpacks and represent diverse environments that can occur

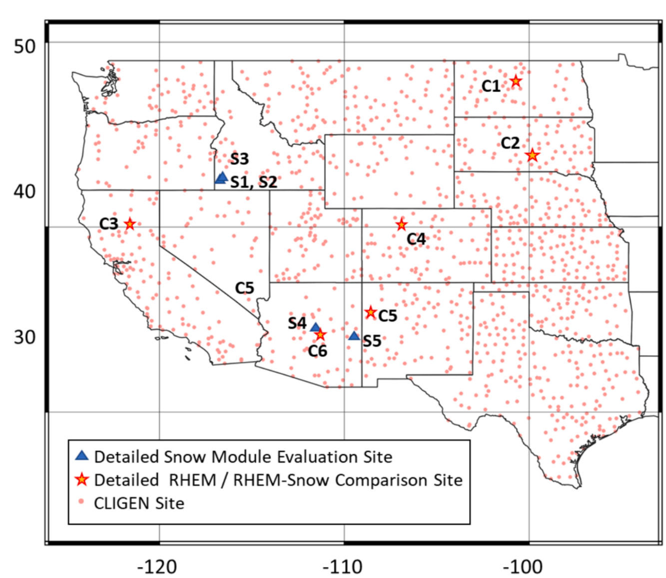

Fig. 1. Site map showing the locations where detailed evaluation of the snow module was conducted (labeled Sites S1–S5) and sites with fully coupled RHEM-Snow simulations that are compared with RHEM simulations and UA snowpack data (1199 sites, 5 of which, labeled C1–C5, include more detailed comparisons than the rest).

in rangeland areas in the western United States.

For each site, the model forcing and validation data include measurements of precipitation, wind speed, air temperature, humidity, solar radiation, snow depth, and SWE (at Sites S1, S4, and S5). At RCEW, these datasets are based on in-situ measurements made by the USDA-ARS in Boise, Idaho. For Sites S1 and S2, these data include a 25-year dataset (from 1984 to 2008) assembled by Reba et al. (2011), and for Site S3, the data (we use data from 2009 to 2019 due to a more limited snow depth observational period at this site) were assembled using data provided through a web portal maintained by the USDA-ARS (https://www.ars.usda.gov/pacific-west-area/boise-id/northwest-watershed-research-center/docs/reynolds-creek-experimental-watershed-data/). At the Arizona sites (Sites S4 and S5), long term snowpack, precipitation, and temperature data are from the Baker Butte and Maverick Fork SNOTELs, and other forcing variables (e.g. relative humidity, solar radiation, wind speed, and pressure) are from the National Land Data Assimilation System (NLDAS) (Xia et al., 2012). All data are aggregated to a daily resolution to match the snow module's timestep.

The stochastic simulations at the 1199 western US CLIGEN sites are driven with 300 years of CLIGEN forcing data (Nicks et al., 1995). Validation data for these tests come from the daily University of Arizona (UA) snowpack dataset (Zeng et al., 2018), which is extracted for the grid cells containing each site. Because of the stochastic nature of the CLIGEN-produced weather data, climatological values (e.g. seasonal snowfall, peak SWE, number of snow-covered days, and first and last day of snow cover) predicted by CLIGEN-forced RHEM-Snow simulations are compared with those from the UA snowpack data (which has 40 years of data). Note that to ensure a match between the snowfall computed from the UA snowpack data (which is taken as the positive daily increments of SWE for each grid cell), we implement a spatially variable rain-snow partitioning method in RHEM-Snow:

$$f_s = \max\left[0, \min\left[1, 1 - \frac{dh}{dx}(T_a - T_{min}) - \frac{dh}{2\pi}\sin\left[\frac{2\pi}{dx}(T_a - T_{min})\right]\right]\right] \quad (5)$$

where T_a is the air temperature, T_{range}, the range over which the rain-snow transition occurs, $T_{max} = T_{mid} + T_{range}/2$ (where T_{mid} is the temperature at which half of the daily precipitation falls as snow), $T_{min} = T_{mid} - T_{range}/2$, $dh = 1$, and $dx = T_{a,max} - T_{a,min}$ (where all terms have units of (°C). This function smoothly transitions from 1 (representing all snowfall) at colder temperatures to zero (representing all rainfall) at warmer temperatures, and it captures the widely observed impact of decreasing snowfall fraction as temperature increases (Dai, 2008; Kienzle, 2008; Marks and Winstral, 2007), including at a site used in this study where precipitation phase is well quantified (Site S1; Fig. S2). Here, the value of T_a is spatially variable and is chosen to ensure that on average, the annual fraction of precipitation that falls as snowfall is the same in RHEM-Snow as is predicted by the UA snowpack dataset. In general, T_a is higher in the Rocky Mountains and Great Plains and lower along the west coast (Fig. S3). Note that all other parameters for the snow module in RHEM-Snow are spatially and temporally constant.

2.3. *Comparing runoff and erosion estimates between RHEM and RHEM-Snow*

To understand the impact of including the snow module on Q and E, we ran RHEM-Snow in two configurations at each site. In the first configuration (called the **Rain-Only, or R_O** configuration, which is the same as RHEM), all precipitation events were treated as rainfall and snowpacks never developed, regardless of the air temperature, and in the second configuration (called the **Rain-Snow, or R_S** configuration, which is the same as RHEM-Snow), some precipitation was considered as snowfall (based on Eq. (5) and the spatially variable T_a shown in Fig. S3), and seasonal snowpacks were allowed to develop. The parameters needed to run the hydrology simulations in RHEM (related to soil texture, slope, and vegetation cover and life form) are derived from USDA Natural Resources Conservation Service's National Resources Inventory (NRI) points that are located close to each CLIGEN site (Nusser and Goebel, 1997; Weltz et al., 2014). Note that RHEM-Snow's snow module also uses these parameters, along with topographic aspect, to model things like the attenuation/enhancement of solar radiation and interception. There are multiple NRI points associated with each CLIGEN site, but we choose parameters from only one NRI point for each CLIGEN site to demonstrate the impact of including the snow module in different regions.

When analyzing the simulation differences, we divided the results based on event type (where each day with rainfall and/or snowmelt was considered as an event):

- **All**: All events
- **R → R:** Events that are categorized as rainfall in both the R_O and R_S configurations when the R_S configuration does not have a snowpack
- **R → S:** Events that are categorized as rainfall in the R_O configuration but where at least some snowfall occurs in the R_S configuration
- **0 → M:** Events that only occur in the R_S configuration because they are caused by snowmelt on days without precipitation
- **R → ROS:** ROS events, where precipitation is considered as rainfall in the R_S configurations when there is snow on the ground

For all categories, we assessed the impact of including the snow module by looking at total changes to runoff and erosion, and the average annual contribution of each event type to total precipitation. For ROS events, we also analyzed changes in runoff and erosion on a per-event basis (by comparing the event-scale changes to event characteristics, e.g. total net water input, changes in peak intensity, pre-existing snowpack). This is because ROS events are unique because they can either enhance or suppress runoff (and also subsequent hillslope erosion) depending on factors such as snowpack thickness and whether the snowpack has enough cold content to freeze rain that falls on it (Marks et al., 1998; Marks et al., 2001).

At six sites, labeled C1-C6 in Fig. 1, we performed a detailed analysis of the overall contributions of each event type and the generated LWI, Q, and E from those events. However, at the remaining sites, we also perform the same coupled simulations, and key metrics (such as LWI, Q, and E differences between R_O and R_S simulations in the different event categories) are mapped across the western US to get an idea of where the inclusion of the snow module makes the largest difference for LWI, Q, and E. Changes in LWI, Q, and E between the Ro and Rs simulations are presented both as a fraction of LWI, Q, and E for each site (as we are particularly interested in how large changes in wintertime LWI, Q, and E changes are relative to total annual values of LWI, Q, and E), as well as absolute differences of LWI, Q, and E.

3. Results

3.1. *Snow module validation*

Fig. 2 shows that RHEM-Snow's snow module is able to reproduce the snowpack dynamics at the two Arizona and three Idaho validation sites. Unsurprisingly, model performance was better at the sites with more substantial and continuous winter snowpacks. For example, at the seasonal snowpack site in Arizona, the R^2 and RMSE between modeled and observed SWE were 0.89 and 42 mm (site S5), while at the ephemeral snowpack site in Arizona, they were 0.73 and 79 mm (site S4). At the Idaho sites, SWE is only measured at the sheltered seasonal snowpack site (site S1), while the exposed seasonal snowpack site and the ephemeral snowpack site (sites S2 and S3) only had snow depth measurements (so only snow depth validation is performed at the latter sites). Compared to the Arizona sites, the sheltered seasonal snowpack site in Idaho also showed favorable model performance ($R^2 = 0.91$; RMSE=73 mm). The performance of the model for snow depth was generally lower than for SWE (note the lower R^2s for snow depth

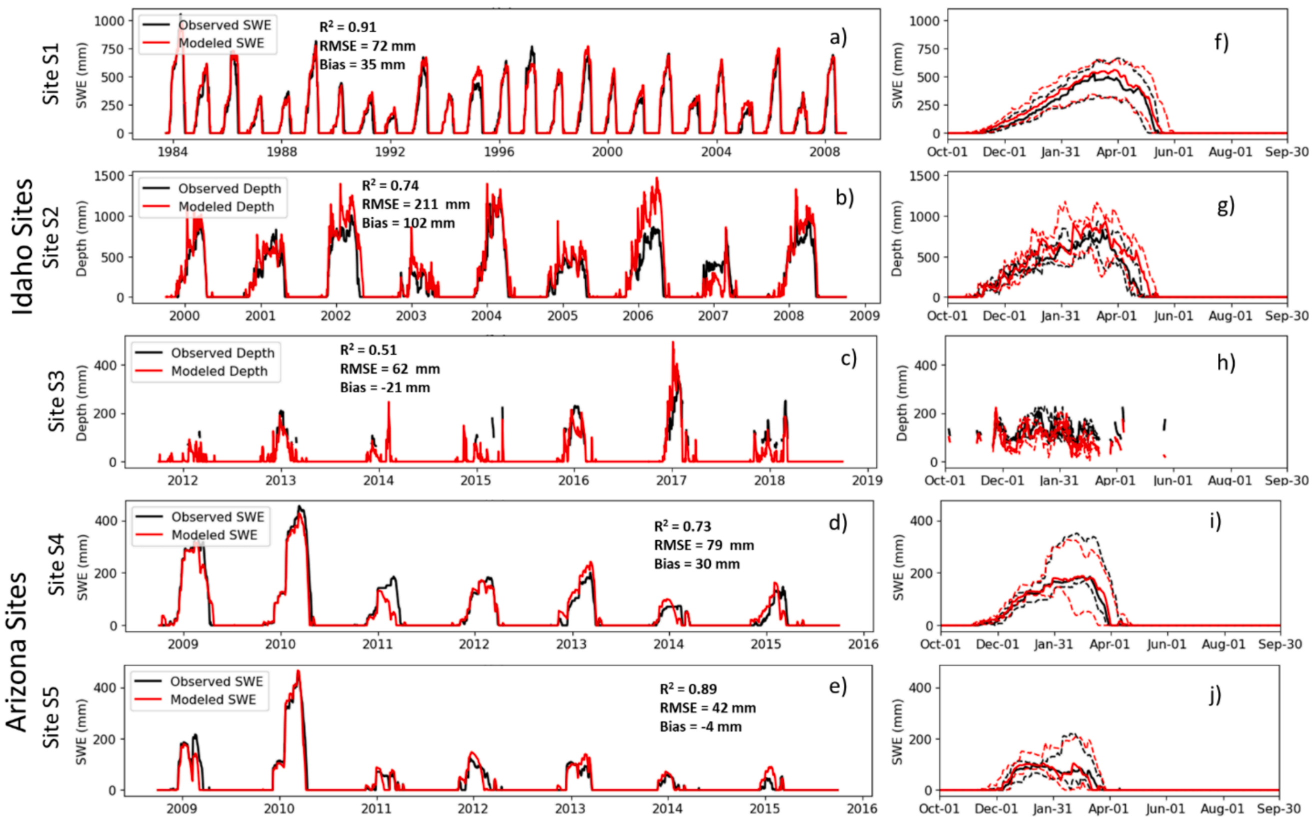

Fig. 2. Comparison between observed and modeled SWE (for Sites 1, 4, and 5) and between observed and modeled snow depth (for Sites S2 and S3; where SWE measurements are unavailable). Panels a)–e) show timeseries' for the period of simulation, and panels f)–j) show seasonal cycles (where the solid lines show the median and dotted lines show the 25th and 75th percentiles).

comparisons in Fig. S4 than for SWE comparisons in Fig. 2 for Sites S1, S4, and S5). However, like the SWE comparison, the agreement was generally better at the sites with deeper snow (compare Fig. 2a with b and c). Note that the annual cycles of SWE and snow depth (e.g. peak SWE, the accumulation period, and the ablation period) are represented well at all sites.

The snow module, when fully integrated into RHEM-Snow and forced with CLIGEN data, is also successful when characterizing the climatological properties of snowpack across the Western US. Fig. 3 shows that compared to UA snowpack data, a variety of characteristics related to the annual cycle of snowpack are represented well. Fig. 3 shows that there is an extremely close correspondence between snowfall, peak SWE, snow cover duration, first snow-covered day, last snow-covered day, and date of peak SWE predicted by RHEM-Snow vs. those from the UA snowpack data (R^2 in all cases is >0.88). There is a slight bias for the first snow-covered day, last snow-covered day, and date of peak SWE (RHEM-Snow, on average, predicts these dates 7–10 days too early), though generally, these differences are small.

3.2. The impact of snow on RHEM's runoff and erosion estimates

Generally, the impact of the snow module on Q and E is limited by how much Q and E occurs in the Ro simulation on days that are either categorized as R → S, 0 → M, or R → ROS, as these days are the ones where the inclusion of the snow module can affect sediment yield and runoff differences. For most sites, Q and E are dominated by summertime events where rainfall events are not reclassified (and hence there is no change between RHEM and RHEM-Snow). For example, for four of the six sites shown in Table 1 (all except for sites C3 and C4), 51–82 % of precipitation falls during R → R events and 72–91 % of Q and 81–93 % of E occur during these events (which is likely due to the higher intensity of summertime precipitation events). For some sites, this leaves little room for change due to the inclusion of snowfall. However, at sites where a higher percentage of Q and E were generated during events that either should have been classified as snowfall or ROS (e.g. Sites 3 and 4, which have most precipitation, Q, and E being produced during the winter), the resulting Q and E could be significantly lower in the Rs simulation, mainly because these quantities were close to zero on R → S days. Note that at these sites, Q and E was relatively small on 0 → M days.

The impact of ROS on Q and E is mixed in the Rs simulation. Note in Table 1 that some sites had more Q and E in the Rs simulation while others had more in the Ro simulation. In addition, the effect of ROS was also mixed for individual ROS events. Fig. 4 shows that on ROS days, Q and E changes are dependent both on whether individual ROS events increased or decreased LWI and whether they changed its intensity. Note that for ROS events which occur over isothermal snowpacks, LWI tends to increase because there is no cold content to freeze the rain to the snowpack, and the warm and potentially windy conditions tend to add additional snowmelt. However, on days when the snowpack is below freezing (i.e., has cold content), it can absorb more energy during the ROS event, including that released by rain freezing to the snowpack, resulting in lower LWI on those days. Note that while total LWI differences between the Ro and Rs simulations are especially highly correlated with Q and E differences between the two simulations, peak intensity differences are also fairly highly correlated with Q and E differences (Fig. 4), underscoring the importance of precipitation (or LWI) intensity for producing Q and E.

3.3. Mapping snow impacts on runoff and erosion across the ConUS

Fig. 5 shows for each event type, the relative differences between LWI from the Ro and Rs simulations across the western continental US (ConUS), relative to total LWI from the Ro simulation. Generally, these relative LWI differences (%ΔLWIs) were larger in the Inner Mountain

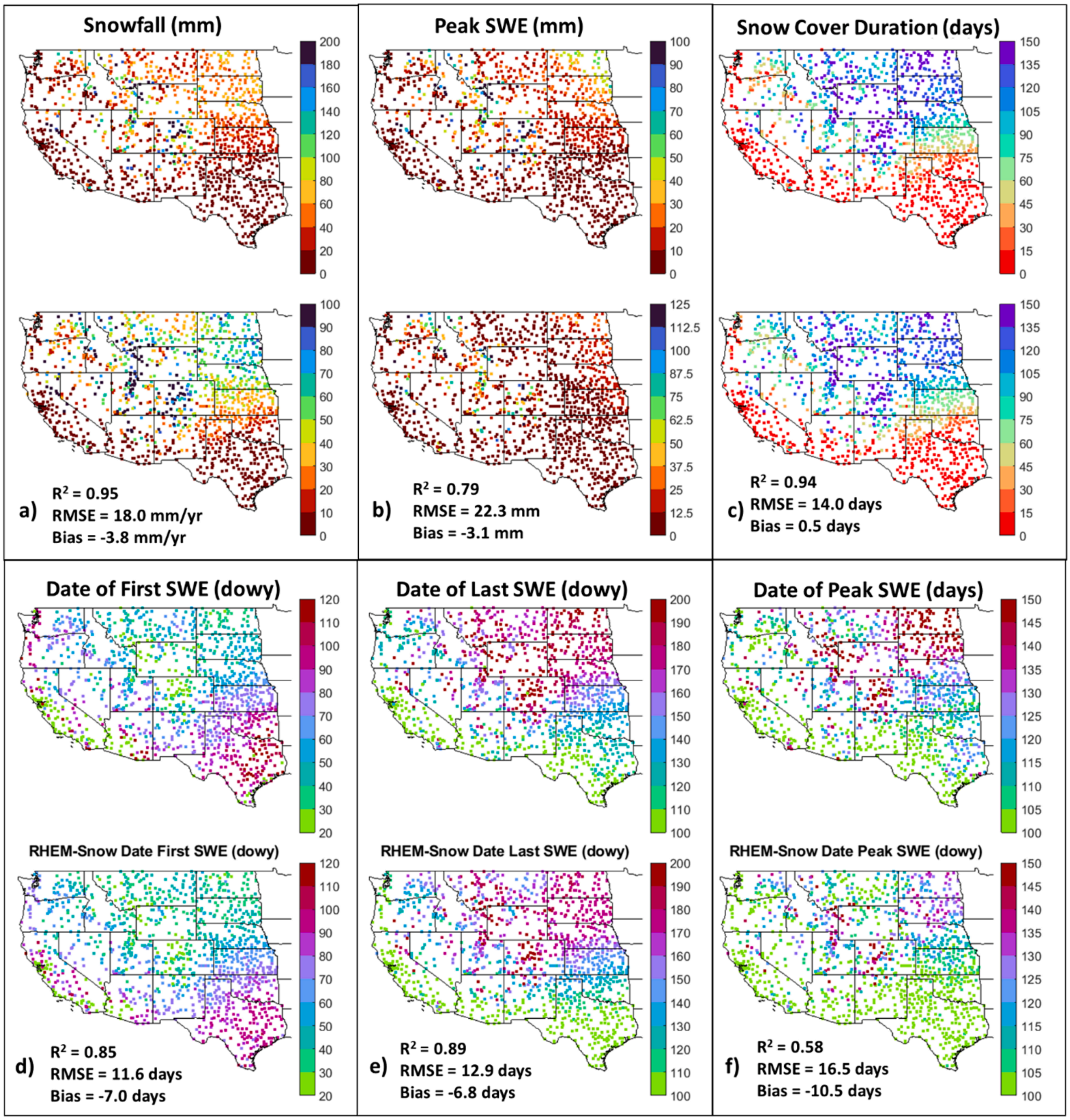

Fig. 3. Comparison between observed and modeled a) and b) average annual snowfall, c) and d) average annual peak SWE, e) and f) average annual snow cover duration, g) and h) average first day of SWE, i) and j) average last day of SWE, k) and l) average date of peak SWE. These dates are given in terms of # of days since October 1st, or day of water year (dowy). Agreement statistics are provided in panels b), d), f), h), j), and l).

West and Upper Great Plains (note that these areas have substantial snowpack accumulations in Fig. 3). The differences can amount to more than 20 % of the total LWI (Fig. 5a), and can be attributed to the sublimation of snow, which is most pronounced in areas where snow persists for a long time (e.g. in the Rocky Mountains), or in areas that have dry, windy climates (e.g. in the Great Basin and Upper Great Plains). When looking at individual event types, reductions of LWI are most dramatic in the Rs simulations for R → S events (up to 40 % of total LWI in some areas), but these reductions are partially made up for during snowmelt (0 → M) events, which, by definition, did not have any water inputs in the Ro simulation. R → ROS events can have either higher or lower LWI in the Rs simulation because ROS is sometimes partly absorbed by the snowpack, and sometimes it melts the snowpack (see Section 3.2). At any rate, the %ΔLWIs are generally smaller than those that occur during R → S, and 0 → M events. Note that to complement Fig. 5, Fig. S5 shows the absolute values of LWI for the Ro simulation, and the absolute values of ΔLWI (which are not scaled by total LWI from the Ro simulation).

Fig. 6 shows the same things as Fig. 5, except for Q instead of LWI. While there are some similarities between the %ΔLWIs in Fig. 5 and the relative Q differences (%ΔQs) in Fig. 6, there are also substantial differences. First, %ΔQs are generally smaller than the %ΔLWIs. In fact, for

Table 1
Average annual precipitation (P), overland flow runoff (Q), and eroded sediment (E) for each event type at the six sites labeled C1-C6 in Fig. 1.

Event type	P (mm/year)	Q_0 (mm/year)	E_0 (kg/ha-year)	ΔQ (mm/year)	ΔE (kg/ha-year)	%ΔQ	%ΔE
	Site C1						
All	531.3	96.2	193.1	−17.1	−16.9	−17.7 %	−8.8 %
R → R	399.9	72.8	167.5	0.0	0.0	0.0 %	0.0 %
R → S	96.2	17.8	17.7	−17.7	−17.6	−18.4 %	−9.1 %
R → ROS	35.2	5.7	7.9	0.4	0.4	0.4 %	0.2 %
0 → M	73.6	0.0	0.0	0.3	0.3	0.3 %	0.2 %
	Site C2						
All	489.7	180.4	3417.6	−10.4	−132.4	−5.8 %	−3.9 %
R → R	404.8	164.3	3197.2	0.0	0.0	0.0 %	0.0 %
R → S	62.4	9.8	117.6	−9.7	−116.6	−5.4 %	−3.4 %
R → ROS	22.5	6.4	102.9	−0.9	−16.6	−0.5 %	−0.5 %
0 → M	22.2	0.0	0.0	0.2	0.8	0.1 %	0.0 %
	Site C3						
All	1303.9	223.8	6887.4	−46.1	−1345.7	−20.6 %	−19.5 %
R → R	289.2	57.9	2103.3	0.0	0.1	0.0 %	0.0 %
R → S	567.7	78.3	2098.9	−78.0	−2089.3	−34.8 %	−30.3 %
R → ROS	446.9	87.5	2680.7	31.3	730.5	14.0 %	10.6 %
0 → M	558.0	0.1	4.2	0.6	13.4	0.3 %	0.2 %
	Site C4						
All	505.4	51.3	450.2	−41.8	−346.2	−81.6 %	−76.9 %
R → R	215.5	6.0	67.0	0.0	0.0	0.0 %	0.0 %
R → S	242.0	41.7	343.0	−41.7	−342.6	−81.2 %	−76.1 %
R → ROS	47.9	3.5	40.0	−0.1	−3.5	−0.3 %	−0.8 %
0 → M	192.2	0.0	0.2	0.0	−0.2	−0.1 %	0.0 %
	Site C5						
All	492.0	64.0	1248.8	−10.1	−134.0	−15.8 %	−10.7 %
R → R	253.8	46.5	1014.0	0.0	0.0	0.0 %	0.0 %
R → S	191.6	11.6	139.6	−11.6	−139.4	−18.1 %	−11.2 %
R → ROS	46.6	5.9	95.2	1.2	4.1	2.0 %	0.3 %
0 → M	120.8	0.0	0.0	0.2	1.3	0.3 %	0.1 %
	Site C6						
All	532.9	158.7	949.2	−10.1	−50.0	−6.4 %	−5.3 %
R → R	409.4	128.8	811.1	−0.1	−0.3	0.0 %	0.0 %
R → S	60.3	13.3	59.9	−13.2	−59.7	−8.3 %	−6.3 %
R → ROS	63.2	16.5	78.1	3.1	10.0	2.0 %	1.0 %
0 → M	41.8	0.0	0.0	0.0	0.0	0.0 %	0.0 %

[1]Note that for 0 → M events, values given in the P column are liquid water inputs from the Rs simulation as by definition, these days had no inputs in the Ro simulation. Q_0 and E_0: Total annual runoff and erosion from the Ro simulation; ΔQ and ΔE: Change in annual runoff and erosion between the Rs and Ro simulations; %ΔQ: ΔQ divided by total annual Q_0 (×100 %); %ΔE: ΔE divided by total annual E_0 (×100 %).

R → S and R → ROS events, %ΔQs are less than half of %ΔLWIs at most sites (compare Figs. 5b-c and 6b-c). Also, snowmelt does not produce much Q (Fig. 6d) in this implementation of RHEM-Snow except for a few sites. As with %ΔLWIs, %ΔQs during R → ROS events are much smaller than %ΔQs for R → S events, so in general, overall reductions of Q are generally attributable to reductions of Q that occurred during R → S events. Note that Q nearly drops to zero during R → S events in the Rs simulation (which can also be seen for the six sites in Table 1). This is because snowfall itself does not cause runoff, but there can still be a little bit of runoff because some rainfall and/or melt can also occur during R → S events (which are defined as having at least some snowfall – see Section 2.2). Similar to Fig. S5, Fig. S6 shows the absolute values of Q for the Ro simulation, and the absolute values of ΔQ between the Ro and Rs simulations. Note, that at many sites ΔQ is relatively small because there is not a lot of Q produced in the first place, even during the summer (Fig. S6). In fact, the amount of Q produced is highly dependent on land cover characteristics (e.g., soils, vegetation cover).

Overall, the spatial maps of relative E differences (%ΔEs), which are shown in Fig. S7, look almost identical to those of the %ΔQs, with the main difference being that the magnitude of %ΔEs are typically a little smaller than %ΔQs (compare Figs. S5g–i and S6g–i). Also, like Q, the absolute values of E are much less spatially consistent than LWI (compare the top panels in Figs. S4–S6), as both Q and E depend heavily on the land cover characteristics of a given site, which are spatially heterogeneous.

To get a sense of the overall reduction of LWI, Q, and E as a function of precipitation amounts for the two event categories where significant changes occur (R → S and R → ROS events), Fig. 7 summarizes %ΔLWI, %ΔQ, and %ΔE for all locations with significant sediment production (>100 kg/ha-yr) as a function of precipitation that falls during R → S and R → ROS events. Unsurprisingly, as snowfall increases, LWI, Q, and E all generally decrease. For example, for sites that receive close to 100 mm of liquid equivalent snowfall per year, annual LWI decreases by ~ 15–40 %, annual Q decreases by 10–30 %, and E decreases by 5–20 % (though keep in mind that absolute Q and E differences depend on how much total annual Q and E are produced in the first place). %ΔLWI, %ΔQ, and %ΔE for R → ROS events are smaller and more variable, but tend to slightly decrease for sites that do not receive much ROS (e.g. those average less than 25 mm of ROS per year) and increase for sites that receive more ROS (e.g., those average less than 100 mm of ROS per year).

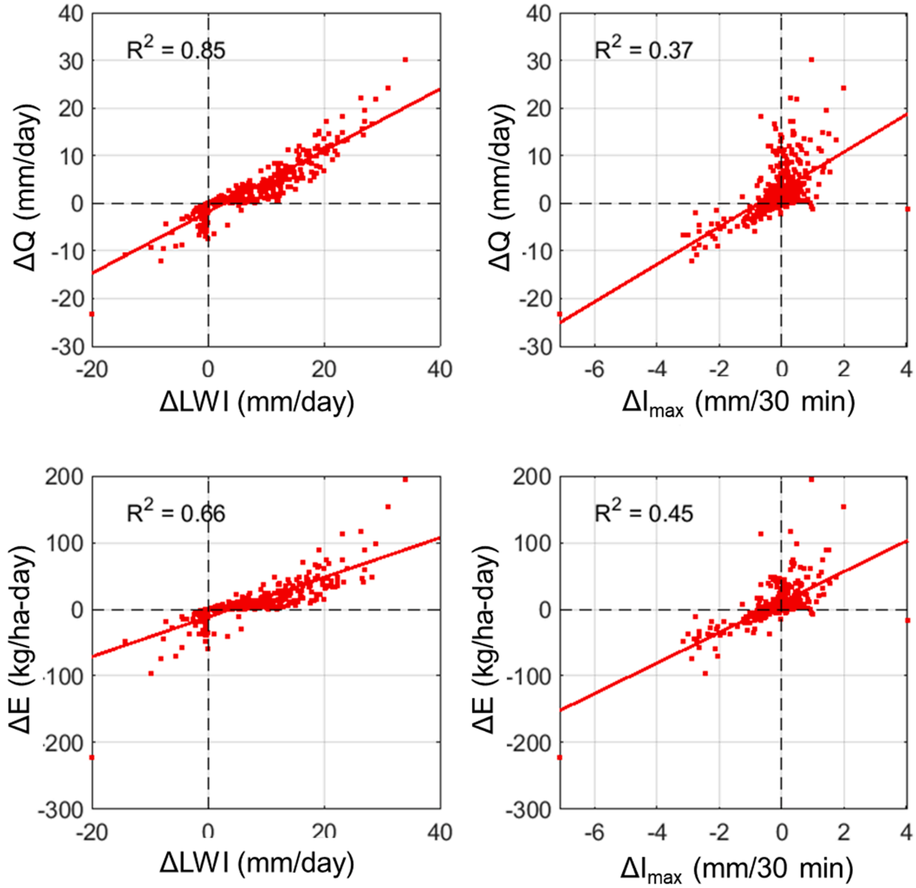

Fig. 4. Relationship between change in liquid water input (ΔLWI) and the maximum 30-min event intensity (ΔI_{max}) and changes in Q and E (ΔQ and ΔE) for ROS events at site C6.

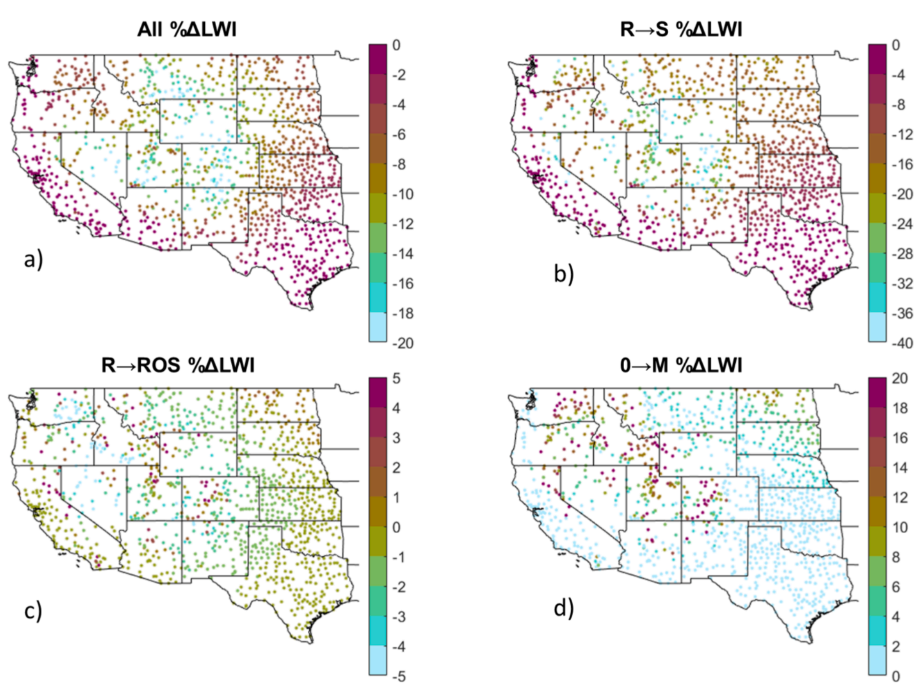

Fig. 5. %ΔLWI, or the average liquid water input difference between the Ro and Rs simulations as a percentage of total LWI from the Ro simulation (×100 %) for All, R → S, R → ROS, and 0 → M events for 1199 CLIGEN sites in the western ConUS. Positive values indicate an increase in LWI in the Rs simulation, and negative values indicate a decrease in LWI in the Rs simulation.

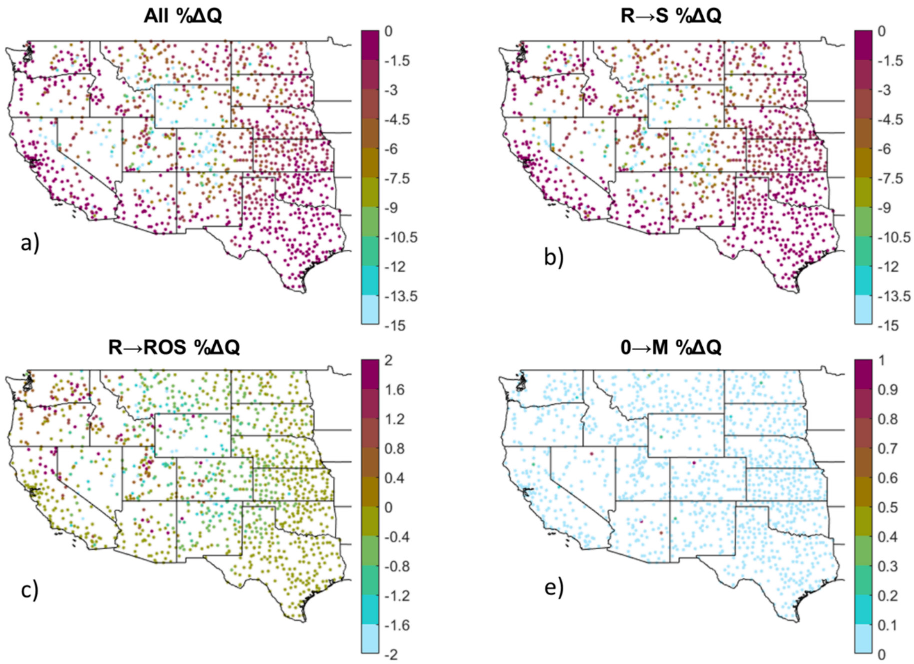

Fig. 6. %ΔQ, or the average surface runoff difference between the Ro and Rs simulations as a percentage of total Q from the Ro simulation (×100 %) for All, R → S, R → ROS, and 0 → M events for 1199 CLIGEN sites in the western ConUS. Positive values indicate an increase in LWI in the Rs simulation, and negative values indicate a decrease in LWI in the Rs simulation.

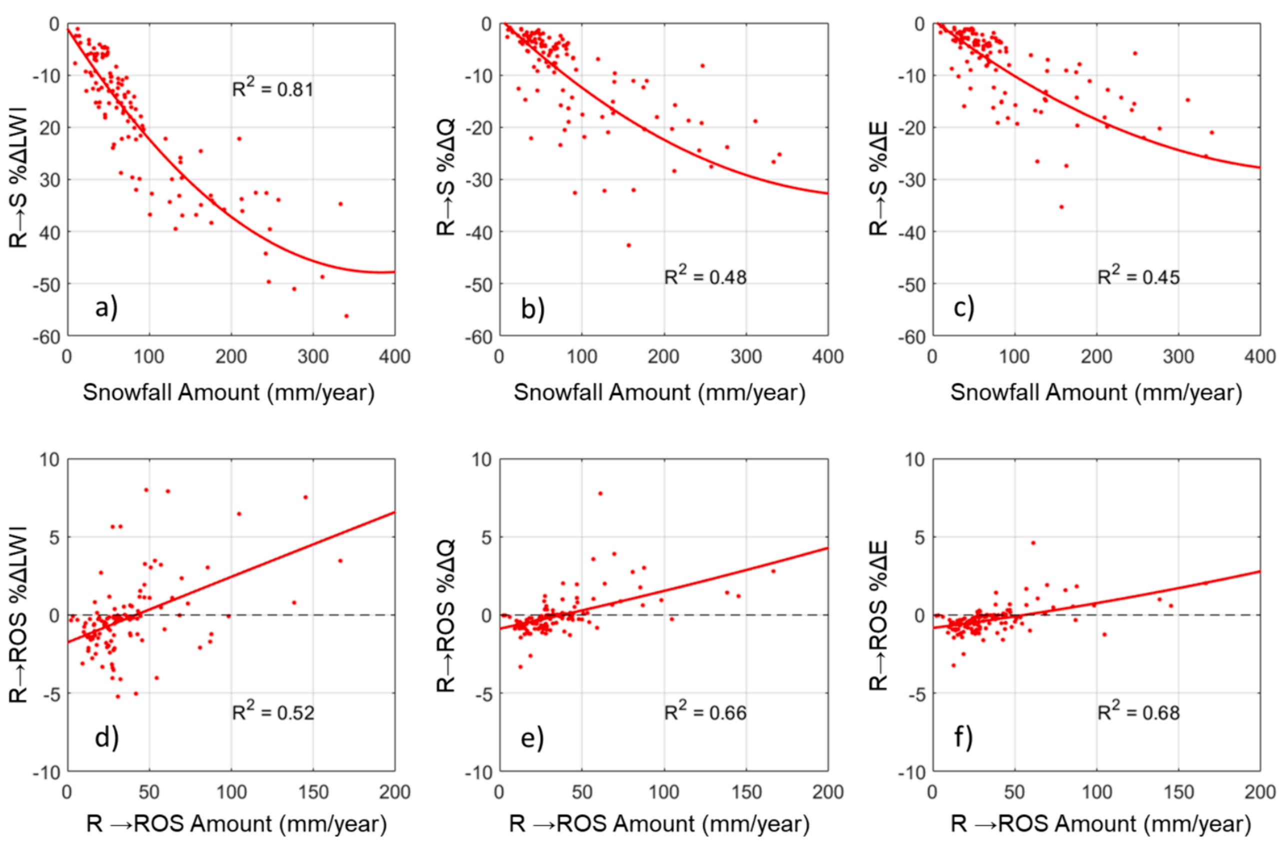

Fig. 7. ΔLWI, ΔQ, and ΔE, as a percentage of total LWI, Q, and E from the Ro simulation for R → S and R → ROS events, plotted against annual average precipitation amounts that occur during these event types.

4. Discussion

In this study, we have addressed a shortcoming of the RHEM model: that all precipitation, regardless of temperature, is treated as rainfall. This can be a problem for areas that receive snowfall because snowmelt has lower intensity than even moderately intense precipitation events and, therefore, produces less Q and E than would occur if the precipitation fell as rain. At the same time though, this impact can be modified by things like frozen or saturated soils. The snow module that we developed is continuous (keeping track of snowpack development and ablation through the winter), yet computationally efficient enough so that it could be implemented as an on-demand model that can be run by rangeland managers to understand vulnerability to erosion. While it is relatively simple (with intermediate complexity between a temperature index snow model and a full energy balance snow model) – it is able to accurately predict snowpack dynamics at test sites (Fig. 2), as well as to reproduce the observed climatological characteristics of snowpack across the ConUS when forced with the same weather simulator data that is used in RHEM (Fig. 3). Furthermore, it does not require additional forcing information than RHEM, making it relatively straight forward to run in an existing decision support framework.

4.1. The impact of treating winter precipitation as snowfall

As expected, including the snow module decreases overland flow runoff and erosion estimates in areas with substantial snowfall. This is primarily due to the reclassification of precipitation events from rainfall to snowfall. While most high-intensity precipitation events occur during the summer when it is warmer, there are regions (such as the Central Rockies) where the large volume of precipitation that occurs as snowfall makes the wintertime precipitation inputs relatively more important for erosion. In these areas, annual Q and E can decrease more than 20 % when considering wintertime precipitation as snowfall (Fig. 7). While the absolute amounts of this decrease are small at many sites due to the fact that not a lot of overland flow runoff and erosion is produced in the first place (Figs. S5 and S6), this reduction can still amount to 10–50 mm/year for overland flow runoff or >100 kg/ha-yr for erosion (Table 1). Not only does some of the snow sublimate to the atmosphere, especially if snowpacks persist for a long time or occur in high energy or arid environments (Fig. 5a), but the subsequent melting of snowpack is less intense than most precipitation.

In fact, in our simulations, snow melting by itself rarely caused enough overland flow to cause erosion. This does not mean, though, that real snowmelt events cannot cause erosion. In fact, in some areas, most streamflow is generated during times of spring snowmelt, and such times can also be associated with large amounts of erosion (Wade and Kirkbride, 1998; Wu et al., 2018). However, during the cool season, lateral subsurface flow (which is not modelled by RHEM) is particularly important (Kelleners et al., 2010; McNamara et al., 2005; Wilcox et al., 1997), leading to channel erosion, which is different than the overland flow-caused erosion that is modeled by RHEM. In addition, the impact of frozen and saturated soils is very important in the winter (which, as noted below, we will address in a future study) (Seyfried and Flerchinger, 1994). In particular, infiltrability can be reduced by repeated cycling between frozen and unfrozen soils (Fouli et al., 2013; Wu et al., 2018), and frozen soil, itself, might be largely impermeable. Infiltrability also decreases for wetter soils (Kane and Stein, 1983), which can be common during the winter due to low evapotranspiration rates, especially in environments where snowpacks are ephemeral (Dwivedi et al., 2023).

Nevertheless, the snow module in RHEM-Snow provides enough complexity to accurately simulate snowmelt under a variety of conditions. It accounts for the impacts of topography (slope and aspect) and vegetation cover on snow accumulation and ablation, and includes representation of many processes that are important for representing snowpack under a variety of conditions (e.g. enhancement/attenuation of solar radiation due to topography, interception, snowpack sublimation). Also, the snow module does a good job representing SWE, both at individual sites when driven with observed forcing data as well as when driven with the stochastic weather generator data that is used in RHEM (Figs. 2 and 3). While the snow module in RHEM-Snow does not explicitly separate SWE into ice water and liquid water, which is typically a few percent or less of SWE, but can be much higher when ice layers are present (Avanzi et al., 2015; Singh et al., 1999), snowmelt leaving the snowpack is still mediated by the accumulation and loss of cold content in the snowpack, resulting in realistic magnitudes of SWE loss (and hence meltout). Furthermore, sub-daily variations in snowmelt are modeled using a beta function that can accurately simulate the daily timing and duration of snowmelt (Webb et al., 2017).

4.2. The impact of rain on snow

ROS events are unique in our simulations, as ROS events can involve enough precipitation with sufficient intensity to generate large amounts of overland flow runoff and sediment production on the hillslopes. In general, though, the presence of snowpack does not necessarily enhance or mute the impact of ROS events (Li et al., 2019; Wever et al., 2014; Würzer et al., 2016). Rather, it depends on precipitation and snowpack characteristics, as shallow, isothermal snowpacks are more likely to melt during ROS events, thereby adding to the LWI. Conversely, deep, cold snowpacks might be able to absorb a substantial amount of precipitation without melting. As a result of this contradictory behavior for individual events, the overall impact of ROS events is somewhat muted in our simulations, and hence the reductions of Q and E that occur due to the reclassification of precipitation from rainfall to snowfall are, overall, more important (Figs. 5–7).

However, similar to snowmelt runoff generation noted above, runoff generation during ROS may be underestimated here because in reality, it is substantially related to the priming of the soil profile for initiating lateral subsurface flow and streamflow in channels (Garvelmann et al., 2015), and the impact of saturated and frozen soils (which is not addressed in the current work) is important for driving runoff and erosion during such events.

4.3. Future work

To address these limitations, future work will focus on updating the subsurface parameterization that is used in RHEM (which currently initialize all events with the same soil saturation and does not allow for frozen soils). Updating this parameterization could potentially have large impacts on overland flow runoff generated during snowmelt, and especially during ROS events, as the current implementation precludes one of the major mechanisms through which ROS causes large amounts of runoff (runoff over frozen soils). Furthermore, runoff efficiencies from ROS events, as well as other events, are heavily linked to catchment wetness and how permeable the soils are. Furthermore, freezing and thawing and excessive wetness can make winter soils more susceptible to erosion (Bajracharya et al., 1998; Wade and Kirkbride, 1998). The impact of variable saturation is likely to extend to the warm season as well, making it a potentially critical issue for erosion modelling given that, in many areas, most Q and E occurs during the warm season.

Along with the continuous snow module described here, we are also working to incorporate a continuous soil hydrology module to keep track of variable soil moisture and frozen soils. However, in this study, we focus on the snowpack portion alone because the variable soil moisture impacts would be present year-round (our focus is just on the impact of snow) and would obscure the impacts of including the snow module (thus limiting our understanding of the impact of snow). In addition, we may also work to address other potential limitations, such as not accounting for wind redistribution of snow, which has been shown to be important for cold, treeless rangeland areas (Winstral and Marks, 2002), but cannot be represented in our current point simulations. Furthermore, future work could also address how to realistically separate solid and liquid components of SWE.

5. Conclusion

Despite these limitations, the current work represents a significant advance for RHEM, as the inclusion of snow module increases the physical realism of the model by correctly partitioning between rainfall and snowfall. This can lead to moderate reductions in annual overland flow runoff and erosion, though in many areas in the western US, this is limited by the relatively small amount of erosion that takes place in RHEM, especially during the winter when precipitation intensities are low. The potential of ROS and rapid snowmelt to cause erosion are likely underestimated due to not including variable saturation and frozen soil effects (which requires an additional module that continuously tracks variable soil moisture and soil freeze–thaw). As such, the reductions in overland flow runoff and erosion found in this study may be reduced, or even reversed once these things are accounted for. Nevertheless, the inclusion of the snow module is an important first step toward simulating more realistic timing and magnitude of overland flow runoff and erosion for cold environments in RHEM.

CRediT authorship contribution statement

Patrick D. Broxton: Writing – original draft, Visualization, Validation, Software, Methodology, Formal analysis, Conceptualization. **David C. Goodrich:** Writing – review & editing, Supervision, Project administration, Funding acquisition, Conceptualization. **D. Phillip Guertin:** Writing – review & editing, Supervision, Project administration, Funding acquisition, Conceptualization. **C. Jason Williams:** Writing – review & editing, Supervision. **Carl Unkrich:** Software, Investigation. **Mariano Hernandez:** Investigation, Data curation. **Andrew Fullhart:** Writing – review & editing, Investigation. **Carrie-Ann Houdeshell:** Writing – review & editing, Project administration. **Mark Seyfried:** Writing – review & editing. **Loretta Metz:** Writing – review & editing, Project administration, Funding acquisition.

Declaration of competing interest

The authors declare that they have no known competing financial interests or personal relationships that could have appeared to influence the work reported in this paper.

Data availability

Data will be made available on request.

Acknowledgements

This material is based upon work supported by the U.S. Department of Agriculture, Natural Resources Conservation Service, Conservation Effects Assessment Project (CEAP) Grazing Lands Component, under agreement number NR193A750007C002. This research was also a contribution from the Long-Term Agroecosystem Research (LTAR) network. The mention of proprietary products does not constitute a guarantee or warranty of the products by USDA or the author and does not imply their approval or the exclusion of other products that may also be suitable.

Appendix A. Supplementary data

Supplementary data to this article can be found online at https://doi.org/10.1016/j.jhydrol.2024.131934.

References

Al-Hamdan, O.Z., Pierson, F.B., Nearing, M.A., Williams, C.J., Hernandez, M., Boll, J., Nouwakpo, S.K., Weltz, M.A., Spaeth, K., 2017. Developing a parameterization approach for soil erodibility for the Rangeland Hydrology and Erosion Model (RHEM). Trans. ASABE 60 (1), 85–94.

Avanzi, F., Yamaguchi, S., Hirashima, H., De Michele, C., 2015. Bulk volumetric liquid water content in a seasonal snowpack: modeling its dynamics in different climatic conditions. Adv. Water Resour. 86, 1–13.

Baffaut, C., Baker, J.M., Biederman, J.A., Bosch, D.D., Brooks, E.S., Buda, A.R., Demaria, E.M., Elias, E.H., Flerchinger, G.N., Goodrich, D.C., 2020. Comparative analysis of water budgets across the US long-term agroecosystem research network. J. Hydrol. 588, 125021.

Bajracharya, R., Lal, R., Hall, G., 1998. Temporal variation in properties of an uncropped, ploughed Miamian soil in relation to seasonal erodibility. Hydrol. Process. 12 (7), 1021–1030.

Blackburn, W.H., Pierson, F.B., Seyfried, M.S., 1990. Spatial and temporal influence of soil frost on infiltration and erosion of sagebrush rangelands 1. JAWRA J. Am. Water Resour. Assoc. 26 (6), 991–997.

Broxton, P., Harpold, A., Biederman, J., Troch, P.A., Molotch, N., Brooks, P., 2015. Quantifying the effects of vegetation structure on snow accumulation and ablation in mixed-conifer forests. Ecohydrology 8 (6), 1073–1094.

Broxton, P.D., van Leeuwen, W.J., Biederman, J.A., 2019b. Improving snow water equivalent maps with machine learning of snow survey and Lidar measurements. Water Resour. Res. 55, 3739–3757.

Broxton, P., Zeng, X., Dawson, N., 2019a. Daily 4 km Gridded SWE and Snow Depth from Assimilated In-Situ and Modeled Data over the Conterminous US, Version 1. NASA National Snow and Ice Data Center Distributed Active Archive Center, Boulder, Colorado USA.

Dai, A., 2008. Temperature and pressure dependence of the rain-snow phase transition over land and ocean. Geophys. Res. Lett. 35 (12).

Demaria, E.M., Dominguez, F., Hu, H., von Glinski, G., Robles, M., Skindlov, J., Walter, J., 2017. Observed hydrologic impacts of landfalling atmospheric rivers in the Salt and Verde river basins of Arizona, United States. Water Resour. Res. 53 (12), 10025–10042.

Dettinger, M.D., Ralph, F.M., Das, T., Neiman, P.J., Cayan, D.R., 2011. Atmospheric rivers, floods and the water resources of California. Water 3 (2), 445–478.

Dwivedi, R., Biederman, J.A., Broxton, P.D., Lee, K., van Leeuwen, W.J. and Pearl, J.K. 2023. Forest density and snowpack stability regulate root zone water stress and percolation differently at two sites with contrasting ephemeral vs. stable seasonal snowpacks. J. Hydrol. 624, 129915.

Flanagan, D.C., Ascough, J.C., Nearing, M.A., Laflen, J.M., 2001. The water erosion prediction project (WEPP) model. Landscape Eros. Evol. Model. 145–199.

Fouli, Y., Cade-Menun, B.J., Cutforth, H.W., 2013. Freeze–thaw cycles and soil water content effects on infiltration rate of three Saskatchewan soils. Can. J. Soil Sci. 93 (4), 485–496.

Fullhart, A.T., Ponce-Campos, G.E., Meles, M.B., McGehee, R.P., Wei, H., Armendariz, G., Burns, S., Goodrich, D.C., 2024. Towards global coverage of gridded parameterization for CLImate GENerator (CLIGEN). Big Earth Data 8 (1), 142–165.

Garvelmann, J., Pohl, S., Weiler, M., 2015. Spatio-temporal controls of snowmelt and runoff generation during rain-on-snow events in a mid-latitude mountain catchment. Hydrol. Process. 29 (17), 3649–3664.

Goodrich, D.C., Broxton, P.D., Guertin, P., Burns, S., Unkrich, C., Korgaonkar, Y., Heilman, P., Hernandez, M., Wei, H., Williams, C.J., 2023. The K2-RHEM-AGWA Suite of Modeling Tools–2023, St Louis, MO.

Havstad, K., Peters, D., Allen-Diaz, B., Bartolome, J., Bestelmeyer, B., Briske, D., Brown, J., Brunson, M., Herrick, J., Huntsinger, L., 2009. The western United States rangelands: a major resource. Grassland Quietness and Strength for a New American Agriculture 75–93.

Hernandez, M., Nearing, M.A., Stone, J.J., Armendariz, G., Pierson, F.B., Al-Hamdan, O. Z., Goodrich, D.C., 2015. Web-based rangeland hydrology and erosion model. Sacramento, CA.

Hernandez, M., Nearing, M.A., Pierson, F.B., Williams, C.J., Spaeth, K.E., Weltz, M.A., 2016. A risk-based vulnerability approach for rangeland management. pp. 1014–1015.

Hernandez, M., Nearing, M.A., Al-Hamdan, O.Z., Pierson, F.B., Armendariz, G., Weltz, M. A., Spaeth, K.E., Williams, C.J., Nouwakpo, S.K., Goodrich, D.C., 2017. The rangeland hydrology and erosion model: a dynamic approach for predicting soil loss on rangelands. Water Resour. Res. 53 (11), 9368–9391.

Kane, D.L., Stein, J., 1983. Water movement into seasonally frozen soils. Water Resour. Res. 19 (6), 1547–1557.

Kelleners, T., Chandler, D., McNamara, J.P., Gribb, M.M., Seyfried, M., 2010. Modeling runoff generation in a small snow-dominated mountainous catchment. Vadose Zone J. 9 (3), 517–527.

Kienzle, S.W., 2008. A new temperature based method to separate rain and snow. Hydrol. Processes: Int. J. 22 (26), 5067–5085.

Lane, L.J., Nearing, M., 1989. USDA-Water Erosion Prediction Project: Hillslope Profile Model Documentation. National Soil Erosion Research Laboratory.

Li, D., Lettenmaier, D.P., Margulis, S.A., Andreadis, K., 2019. The role of rain-on-snow in flooding over the conterminous United States. Water Resour. Res. 55 (11), 8492–8513.

Liston, G.E., Elder, K., 2006. A distributed snow-evolution modeling system (SnowModel). J. Hydrometeorol. 7 (6), 1259–1276.

Marks, D., Winstral, A., 2007. Finding the rain/snow transition elevation during storm events in mountain basins.

Marks, D., Kimball, J., Tingey, D., Link, T., 1998. The sensitivity of snowmelt processes to climate conditions and forest cover during rain-on-snow: a case study of the 1996 Pacific Northwest flood. Hydrol. Process. 12 (10–11), 1569–1587.

Marks, D., Link, T., Winstral, A., Garen, D., 2001. Simulating snowmelt processes during rain-on-snow over a semi-arid mountain basin. Ann. Glaciol. 32, 195–202.

Mazurkiewicz, A.B., Callery, D.G., McDonnell, J.J., 2008. Assessing the controls of the snow energy balance and water available for runoff in a rain-on-snow environment. J. Hydrol. 354 (1–4), 1–14.

McNamara, J.P., Chandler, D., Seyfried, M., Achet, S., 2005. Soil moisture states, lateral flow, and streamflow generation in a semi-arid, snowmelt-driven catchment. Hydrol. Processes: Int. J. 19 (20), 4023–4038.
Meusburger, K., Leitinger, G., Mabit, L., Mueller, M., Walter, A., Alewell, C., 2014. Soil erosion by snow gliding–a first quantification attempt in a subalpine area in Switzerland. Hydrol. Earth Syst. Sci. 18 (9), 3763–3775.
Nayak, A., Marks, D., Chandler, D., Seyfried, M., 2010. Long-term snow, climate, and streamflow trends at the Reynolds Creek experimental watershed, Owyhee Mountains, Idaho, United States. Water Resour. Res. 46 (6).
Nearing, M., Pruski, F., O'neal, M., 2004. Expected climate change impacts on soil erosion rates: a review. J. Soil Water Conserv. 59 (1), 43–50.
Nearing, M., Wei, H., Stone, J., Pierson, F., Spaeth, K., Weltz, M., Flanagan, D., Hernandez, M., 2011. A rangeland hydrology and erosion model. Trans. ASABE 54 (3), 901–908.
Nicks, A., Lane, L. and Gander, G. 1995. Ch. 2. Weather generator. USDA-Water Erosion Prediction Project: Hillslope Profile and Watershed Model Documentation.
Nusser, S.M., Goebel, J.J., 1997. The National Resources Inventory: a long-term multi-resource monitoring programme. Environ. Ecol. Stat. 4, 181–204.
Reba, M.L., Marks, D., Seyfried, M., Winstral, A., Kumar, M., Flerchinger, G., 2011. A long-term data set for hydrologic modeling in a snow-dominated mountain catchment. Water Resour. Res. 47 (7).
Seyfried, M., Flerchinger, G., 1994. Influence of frozen soil on rangeland erosion. Variability in Rangeland Water Erosion Processes 38, 67–82.
Seyfried, M., Lohse, K., Marks, D., Flerchinger, G., Pierson, F., Holbrook, W.S., 2018. Reynolds creek experimental watershed and critical zone observatory. Vadose Zone J. 17 (1), 1–20.
Seyfried, M.S., Wilcox, B., 1995. Scale and the nature of spatial variability: field examples having implications for hydrologic modeling. Water Resour. Res. 31 (1), 173–184.
Singh, P., Spitzbart, G., Huebl, H., Weinmeister, H., 1999. Importance of ice layers on liquid water storage within a snowpack. Hydrol. Process. 13 (12–13), 1799–1805.
Srivastava, A., Flanagan, D., Frankenberger, J., Engel, B., 2019. Updated climate database and impacts on WEPP model predictions. J. Soil Water Conserv. 74 (4), 334–349.
Wade, R., Kirkbride, M., 1998. Snowmelt-generated runoff and soil erosion in Fife, Scotland. Earth Surf. Processes Landforms 23 (2), 123–132.
Walthall, C., Hatfield, J., Backlund, P., Lengnick, L., Marshall, E., Walsh, M., Adkins, S., Aillery, M., Ainsworth, E., Ammann, C., 2012. Climate Change and Agriculture in the United States: Effects and Adaptation.
Webb, R.W., Fassnacht, S.R., Gooseff, M.N., 2017. Defining the diurnal pattern of snowmelt using a beta distribution function. JAWRA J. Am. Water Resour. Assoc. 53 (3), 684–696.
Wei, X., Huang, C., Wei, N., Zhao, H., He, Y., Wu, X., 2019. The impact of freeze–thaw cycles and soil moisture content at freezing on runoff and soil loss. Land Degrad. Dev. 30 (5), 515–523.
Wei, H., Nearing, M., Stone, J., 2007. A comprehensive sensitivity analysis framework for model evaluation and improvement using a case study of the rangeland hydrology and erosion model. Trans. ASABE 50 (3), 945–953.
Weltz, M.A., Jolley, L., Hernandez, M., Spaeth, K.E., Rossi, C., Talbot, C., Nearing, M., Stone, J., Goodrich, D., Pierson, F., 2014. Estimating conservation needs for rangelands using USDA National Resources Inventory assessments. Trans. ASABE 57 (6), 1559–1570.
Wever, N., Jonas, T., Fierz, C., Lehning, M., 2014. Model simulations of the modulating effect of the snow cover in a rain-on-snow event. Hydrol. Earth Syst. Sci. 18 (11), 4657–4669.
Wilcox, B.P., Newman, B.D., Brandes, D., Davenport, D.W., Reid, K., 1997. Runoff from a semiarid ponderosa pine hillslope in New Mexico. Water Resour. Res. 33 (10), 2301–2314.
Williams, C.J., Pierson, F.B., Spaeth, K.E., Brown, J.R., Al-Hamdan, O.Z., Weltz, M.A., Nearing, M.A., Herrick, J.E., Boll, J., Robichaud, P.R., 2016. Incorporating hydrologic data and ecohydrologic relationships into ecological site descriptions. Rangel. Ecol. Manage. 69 (1), 4–19.
Williams, C.J., Pierson, F.B., Al-Hamdan, O.Z., Nouwakpo, S.K., Johnson, J.C., Polyakov, V.O., Kormos, P.R., Shaff, S.E., Spaeth, K.E., 2022. Assessing runoff and erosion on woodland-encroached sagebrush steppe using the Rangeland Hydrology and Erosion Model. Ecosphere 13 (6), e4145.
Winstral, A., Marks, D., 2002. Simulating wind fields and snow redistribution using terrain-based parameters to model snow accumulation and melt over a semi-arid mountain catchment. Hydrol. Process. 16 (18), 3585–3603.
Wu, Y., Ouyang, W., Hao, Z., Yang, B., Wang, L., 2018. Snowmelt water drives higher soil erosion than rainfall water in a mid-high latitude upland watershed. J. Hydrol. 556, 438–448.
Würzer, S., Jonas, T., Wever, N., Lehning, M., 2016. Influence of initial snowpack properties on runoff formation during rain-on-snow events. J. Hydrometeorol. 17 (6), 1801–1815.
Xia, Y., Mitchell, K., Ek, M., Sheffield, J., Cosgrove, B., Wood, E., Luo, L., Alonge, C., Wei, H., Meng, J., 2012. Continental-scale water and energy flux analysis and validation for the North American Land Data Assimilation System project phase 2 (NLDAS-2): 1. Intercomparison and application of model products. J. Geophys. Res. Atmos. 117 (D3).
Zeng, X., Broxton, P., Dawson, N., 2018. Snowpack change from 1982 to 2016 over conterminous United States. Geophys. Res. Lett. 45 (23), 12,940–912,947.
Zhang, X., Garbrecht, J.D., 2003. Evaluation of CLIGEN precipitation parameters and their implication on WEPP runoff and erosion prediction. Trans. ASAE 46 (2), 311.
Zhang, Y., Hernandez, M., Anson, E., Nearing, M., Wei, H., Stone, J., Heilman, P., 2012. Modeling climate change effects on runoff and soil erosion in southeastern Arizona rangelands and implications for mitigation with conservation practices. J. Soil Water Conserv. 67 (5), 390–405.